American Mineralogist, Volume 90, pages 173–180, 2005

Dehydroxylation and CO_2 incorporation in annealed mica (sericite): An infrared spectroscopic study

MING ZHANG,[1,*] LING WANG,[2] SHIGETO HIRAI,[3] SIMON A.T. REDFERN,[1] AND EKHARD K.H. SALJE[1]

[1]Department of Earth Sciences, University of Cambridge, Downing Street, Cambridge CB2 3EQ, U.K.
[2]College of Materials and Bioengineering, Chengdu University of Technology, Chengdu 610059, Sichuan, P. R. China
[3]Department of Applied Physics and Physico-informatics, Keio University, Yokohama, Japan

ABSTRACT

Dehydroxylation and incorporation of CO_2 in mica (sericite-$2M_1$) during high-temperature annealing has been investigated in detail using infrared (IR) spectroscopy. The dehydroxylation is characterized by a dramatic change of the OH^- ion spectrum and the appearance or development of different extra species (CO_2, CO_3^{2-}, and OH^-). A significant decrease in the K-O bond strength and a complex distortion of the silicon-oxygen tetrahedra were also observed. The general similarities between the spectra of the untreated and dehydroxylated sericite show that the layered framework is somewhat preserved in sericite dehydroxylate. The results suggest that the incorporation of CO_2 into the structures of the heated materials is associated with or enhanced by the dehydroxylation process, although the two processes have different reaction mechanisms. The CO_2 contents in heat-treated sericite show a correlation with the loss rate of hydroxyl. A weak O-H stretching absorption band near 3480 cm^{-1} developed during dehydroxylation and it disappeared above 1100 °C. The results suggest that the developed additional O-H stretching signals and the thermally induced CO_2 do not structurally stabilize each other, as upon further heating the two different types of components vanished at different temperatures.

INTRODUCTION

Mica minerals constitute the most abundant ferromagnesian phase encountered in magmatic, metamorphic, and hydrothermal ore deposits. They belong to a family of minerals known as phyllosilicates, which are composed of sheets of silicate tetrahedra. Micas are generally known for their thermal stability, high resistance, uniform dielectric constant/capacitance stability, and low power loss, and consequently are used extensively in electronic devices. They have been recently utilized for polymer/layered silicate nanocomposites (Ray and Okamoto 2003) and substrates for epitaxial growths of sexiphenyl thin films (e.g., Plank et al. 2003). In geology, cation releases in natural micas are commonly studied to investigate hydrothermal alteration and weathering processes (e.g., Kapoor et al. 1981; Taylor et al. 2000). Mica is also a phase used for isotope age dating (e.g., Copeland and Harrison 1990) and alpha-decay recoil track analysis (e.g., Hashemi-Nezhad and Durrani 1981; Glasmacher et al. 2003).

Dehydroxylation in clay minerals has been the subject of many investigations. The present study was inspired by the question: what happens at the atomic level during dehydroxylation in 2:1 layer silicates? Although different mechanisms for the dehydroxylation process have been proposed (MacKenzie et al. 1985; Guggenheim et al. 1987; Drits et al. 1995; Fitzgerald et al. 1996; Muller et al. 2000; Wang et al. 2002), the issue is still under debate. We wished to investigate in detail the spectral changes related to different vibrational bands (e.g., these of O-H, K-O, Si-O, Al-O vibrations) and to compare IR data from OH^- species with those obtained through other analytical methods, especially those from thermogravimetric measurements, for the purpose of gaining a better understanding of the dehydroxylation process.

The present study was also motivated by our recent observation of incorporated carbon species in partially dehydroxylated pyrophyllite (Wang et al. 2003), and we wished to further investigate this issue. The incorporation of CO_2 into minerals and glasses has previously been reported as part of studies of CO_2 solubility in melts (e.g., Mysen 1976; Fine and Stolper 1985; Taylor 1990; Brooker et al. 1999, 2001; Béarat et al. 2002; Morizet et al. 2002). CO_2 contents and their molecular speciation in minerals can offer information on the formation condition and geological history of the rocks in which they occur. An understanding of the solubility and stability mechanisms of CO_2 in silicate melts is of significance and interest in geology because of the important role CO_2 plays in the petrogenesis of a wide range of igneous rocks. The incorporation of CO_2 into pyrophyllite [$Al_2Si_4O_{10}(OH)_2$] during dehydroxylation has been reported recently (Wang et al. 2003), along with an intermediate phase. The observations in our previous study on pyrophyllite have led to several important fundamental questions: do other phyllosilicate clays show similar behaviors at high temperatures? Is the incorporation of CO_2 associated with the dehydroxylation process? If yes, how or to what extent are they related? Although the physics behind the CO_2 incorporation in melts or glasses may be different from that in heated clays, a better understanding of the process may provide additional insights for other researchers. For instance, it may offer useful information on sequestration of anthropogenic gases in natural (mineral) sinks and during production of fired clay materials, and also to those workers who observed carbon dioxide released during thermal analysis

* E-mail: mz10001@esc.cam.ac.uk

0003-004X/05/0001–173$05.00/DOI:10.2138/am.2005.1615

of clays in air which could not be explained by dissociation of carbonates or oxidation of organic matter.

In the present study, we report our newly recorded experimental data for dehydroxylation and the incorporation of CO_2 in sericite (a fine-grained variety of muscovite), which is a dioctahedral clay mineral with a general chemical formula of $(K,Na)Al_2[AlSi_3O_{10}](OH)_2$. The material was chosen for this study not only because of the sample availability and quality, but also because muscovite and pyrophyllite have similar structures (Deer et al. 1992) and they are generally believed to have similar dehydroxylation behaviors (e.g., Guggenheim et al. 1987). In the present study, the CO_2 species was used as a structural probe and the results offer some insights into local changes during dehydroxylation, and help to clarify some contradictory issues regarding different dehydroxylation models.

Experimental methods

The sample ($2M_1$) used in the present study is from the sericite deposit in Song County, Henan Province, China, with a characteristic chemical composition (wt%) of SiO_2 46.19, Al_2O_3 35.35, Fe_2O_3 0.96, TiO_2 0.68, CaO 0.30, MgO 0.78, K_2O 9.91, Na_2O 0.37, and H_2O 4.75 (Pei and Shi 1996). Both powdered (with grain sizes of a few micrometers) and thin section (with thickness of ~245 μm) samples were used in the experiments. Because sericite is relatively soft, the powdered samples were obtained by gently grinding in an agate mortar, whereas the thin sections were chopped from a large crystal, flatted with coarse cloth, and then polished with commercial polishing cloth. No organic or inorganic solutions, waxes and glues, which could potentially lead to sample contamination, were used in the sample preparation process.

The thermal annealing of the sericite sample was carried out between 300 and 1400 °C in a Lenton furnace in air at one atmosphere. The furnace was pre-heated to a set temperature before sample loading and the samples were annealed for 15 min (for the thin sections) or 1 hr (for powdered samples). The annealing time was chosen to gain a better understanding of the effect of temperature on the samples. The annealed samples were quenched onto lab benches in air. Fresh sample powders were used for thermal treatments at different temperatures, however, thermally treated thin sections were annealed at a higher temperature after being measured at room temperature. The pellet technique reported by Zhang et al. (1996) was used to measure the powdered samples. Polyethylene and KBr powders were used as matrix materials (sample:matrix = 1:50 for polyethylene, and 1:300 or 1:100 for KBr). The sample/matrix mixtures were pressed into disc-shaped pellets 13 mm in diameter at room temperature under vacuum. The sample pellets prepared with KBr were then stored in an oven (150 °C) for two hours to remove possible absorbed surface water. All sample pellets were measured within 12 hours of creation.

Absorption spectra (in the wavenumber region of 20–5000 cm^{-1}) of powdered sample pellets were recorded using a Bruker IFS 113v spectrometer. An Hg lamp, a DTGS detector, 12 μm and Ge-coated 6 μm Mylar beamsplitters were used for far-IR measurements, whereas a globar lamp, a KBr beamsplitter, and a DTGS detector were chosen for mid-IR. Absorption spectra (2000–13 000 cm^{-1}) of the thin section sample were acquired at room temperature using a Bruker IFS 66v spectrometer. Apertures of 1.0–2.5 mm, a tungsten lamp, a liquid-nitrogen-cooled mercury-cadmium-telluride detector, and a CaF_2 beam-splitter were used. A total of 512 scans were collected for each spectrum. Instrumental resolutions of 2 and 4 cm^{-1} were used. All spectra were collected under vacuum. Data analysis was carried out using commercial software (OPUS-IR II, Bruker). Integrated absorbance was obtained by curve fitting or simply by integrating the measured data with linear base lines.

Results

The infrared spectra of sericite show vibrational bands of the layer structure between 20 and 4000 cm^{-1} (Figs. 1a and 1b). Some band assignments on mica and other layer silicates have been previously documented (Farmer and Russell 1964; Ishii et al. 1967; Farmer 1974; Langer et al. 1981; Laperche and Prost 1991; Robert et al. 1993; McKeown et al. 1999; Diaz et al. 2000, 2002; Beran 2002). The bands between 90 and 200 cm^{-1} in sericite (or muscovite) are mainly due to K-O vibrations (Diaz et al. 2002). Our data did not reveal any IR bands between 20 and 90 cm^{-1}. The bands between 300 and 550 cm^{-1} can be simply considered as bending vibrations of SiO_4 and AlO_6. The bands between 900 and 1200 cm^{-1} are mainly attributed to stretching vibrations of the SiO_4 group and the stretching due to T-O-T (T = Si/Al) vibrations, whereas the band near 920 cm^{-1} is attributed to

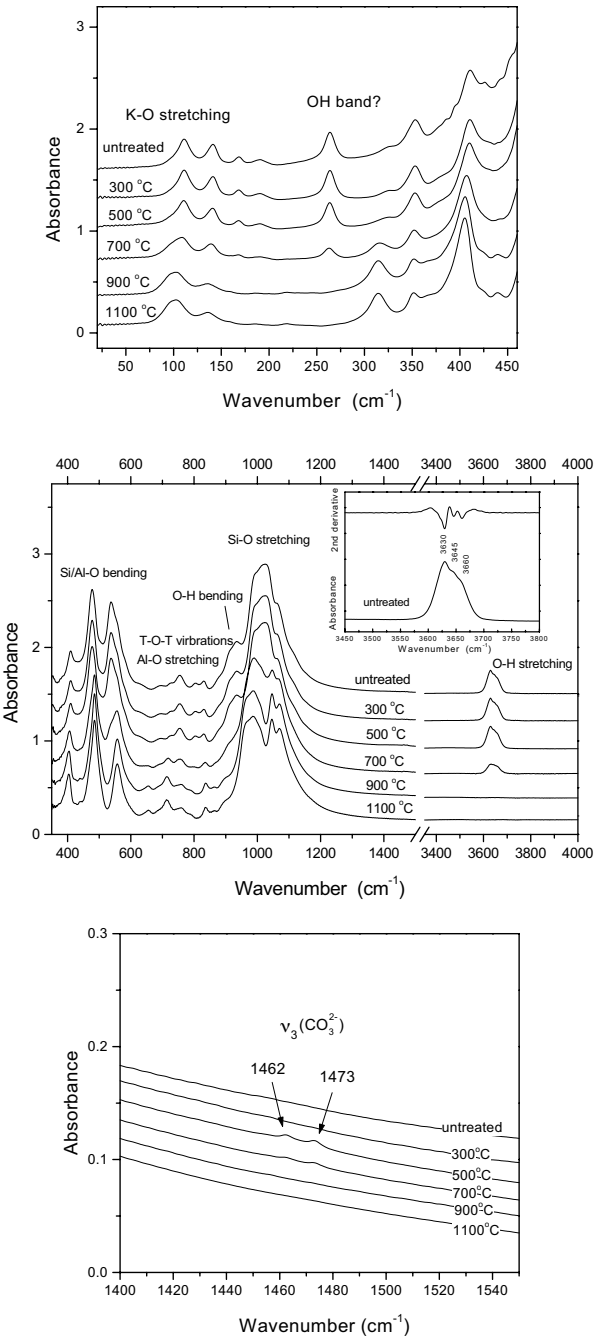

Figure 1. Temperature evolution of vibrational bands of sericite: (**a**) 20–450 cm^{-1} (from polyethylene pellets), (**b**) 350–4500 cm^{-1} (obtained from KBr pellets), and (**c**) 1400–1550 cm^{-1} (obtained from KBr pellets). The spectra are shifted for clarity.

the libration motion (δ-OH) of the OH^- species. Vibrations related to Al-O stretching, tilting motion of the base of the tetrahedron, and T-O-T bending bands are mainly located between 700 and 850 cm^{-1}. The untreated sample did not contain CO_3^{2-} and CO_2 species as evidenced by the lack of their characteristic absorption signals between 1400 and 1500 cm^{-1} and near 2345 cm^{-1} (Figs. 1c and 2). The structurally incorporated hydroxyl groups in sericite show O-H stretching bands near 3630, 3645, and 3660 cm^{-1} (Figs. 1b and 3a). The features near 4108, 4265, and 4555 cm^{-1} (Fig. 4) have complex origins and are mainly attributed to combinations of the O-H stretching bands with other OH^- vibrations (e.g., the OH^- libration near 920 cm^{-1}), and probably with framework phonons, e.g., the stretching and bending of AlO_6 and SiO_4 (Fig. 1b), as these bands between 4100 and 4600 cm^{-1} disappeared in the sericite dehydroxylate. The features between 7050 and 7200 cm^{-1} (Fig. 5) are assigned as the first overtones of the O-H stretching bands near 3630 cm^{-1}.

The dehydroxylation in sericite is evidenced by a dramatic decrease in intensity in the O-H stretching bands between 3630 and 3660 cm^{-1} (Figs. 1b and 3a). Similar changes in this wavenumber region were reported previously (Gaines and Vedder 1964; Aines and Rossman 1985). Our IR data for the OH overtones near 7050 and 7200 cm^{-1} exhibit a thermal behavior identical to their fundamental bands (Fig. 5). Heating led to little spectral variation below 400 °C. A decrease of OH intensity commenced near 500 °C (Figs. 6a–c). With further heating, the water loss rate reaches a maximum near 700 °C as shown in Figure 6c, where the negative value of the change (the derivative) of the OH^- integral absorbance indicates decreasing signals. The flat lines shown by the samples annealed at temperatures higher than 900 °C (Figs. 3a and 5) indicate that the original OH^- species between 3630 and 3660 cm^{-1} have vanished at these temperatures. This observation is further supported by the disappearance of the combination bands between 4000 and 4700 cm^{-1} (Fig. 4). We noted that the dehydration did not cause significant change in the OH^- ion band frequency. For instance, the bands near 3630 and 3640 cm^{-1} showed no detectable shift after the sample was annealed at 800 °C (Fig. 3a). This finding appears to suggest that in dehydroxylation the bonding associated with these OH^- species does not become significantly weaker or stronger. In addition, their widths exhibit weak changes. In the untreated sample, the spectral feature between 3600 and 3700 cm^{-1} (consisting of the three O-H stretching bands) gives an "overall" width of ~60 cm^{-1} (Fig. 1b). After being annealed at 800 °C, the sample showed a value of ~63 cm^{-1}. In an in situ IR study of dehydroxylation in muscovite, Aines and Rossman (1985) observed a more significant variation (~28 cm^{-1}) in the O-H stretching band frequency. The differences between these two studies could be due to different measurement conditions (in situ high temperature measurements vs. room-temperature measurements of quenched samples). Thus, temperature-induced band shift and lattice expansion might partially or fully account for the difference. This interpretation is further supported by in situ IR measurements of sericite at low temperatures, which show that cooling from 300 to 20 K leads to a change of 5 cm^{-1} in the O-H stretching band frequency (Zhang et al. in preparation). We noted with interest that a broad shoulder near 3444 cm^{-1} (Figs. 3a and 3b), which appeared in the thin section sample (it is too weak to be seen in powder absorption measurements) and whose origin is unclear, gradually vanished on heating to near 550 °C and an absorption band near 3480 cm^{-1} developed

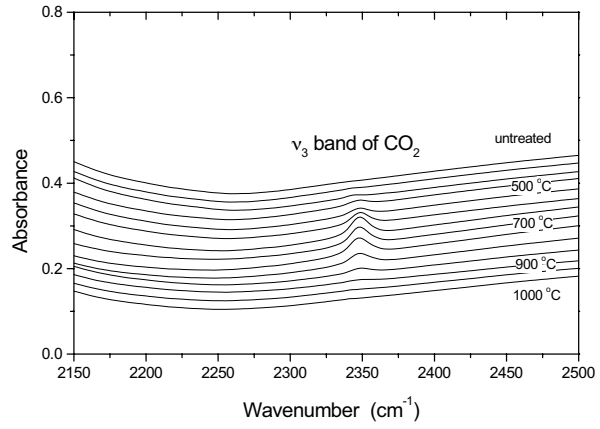

FIGURE 2. Temperature evolution of CO_2 spectra (data from thin sections) between 2150 and 2500 cm^{-1}. The spectra are shifted for clarity.

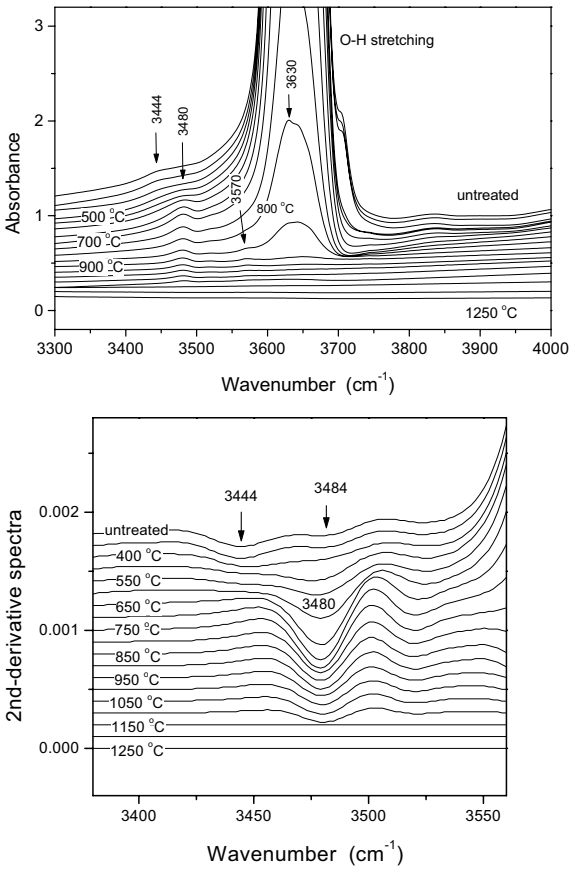

FIGURE 3. Temperature evolution of hydroxyl spectra between 3300 and 4000 cm^{-1} (data from thin sections). (**a**) Absorption spectra. (**b**) Second derivate spectra (between 3360 and 3640 cm^{-1}). The additional signal near 3480 cm^{-1} appeared between 500 and 1100 °C.

at temperatures as low as ~500 °C (this band might or might not be associated with the almost undetectable weak absorption near 3484 cm^{-1} in the starting material, which also showed systematic intensity decrease from room temperature to 400 °C). The frequency of this 3480 cm^{-1} feature is consistent with the stretching vibrations of OH^- species, but it is too high for possible N-H stretching (commonly at ~3200 cm^{-1}) associated with NH_4. This absorption gained intensity with increasing temperature, and it became sharper (Figs. 3a and 3b). Its absorption reached a maximum near 700 °C and became progressively weaker on further heating. Although the main OH^- features near 3630 and 3660 cm^{-1} had already disappeared at temperatures near 900 °C, the feature near 3480 cm^{-1} was present at temperatures as high as 1100 °C. It finally disappeared in the sample annealed at 1150 °C. Another weak absorption near 3570 cm^{-1} was recorded in the sample treated at 850 °C (Fig. 3a) and its frequency suggests that it is due to O-H stretching vibrations. The development of these features probably indicates the migration of protons and a thermally induced local structural modification, which probably results in the formation of new structural sites. The disappearance of the bands at much higher temperatures, in comparison to those hydroxyl bands between 3630 and 3660 cm^{-1}, suggests that these OH^- species could have higher activation energies.

The effect of dehydroxylation on the crystal structure of sericite is also shown by significant changes in the vibrational spectrum between 20 and 1500 cm^{-1} (Figs. 1a and 1b), where the phonon bands from the layered structure as well as some OH^- bands are located. The effect is characterized by changes in band intensity and frequency. The OH^- libration band near 920 cm^{-1} shows decreasing in intensity above 500 °C and vanishes in the sericite dehydroxylate. The disappearance of the relatively intense band near 260 cm^{-1} suggests that it might be mainly or partially associated with OH^- vibration. As shown in Figures 1a and 1b, sericite and its dehydroxylate exhibit similar overall spectral patterns. This implies that the local structure associated

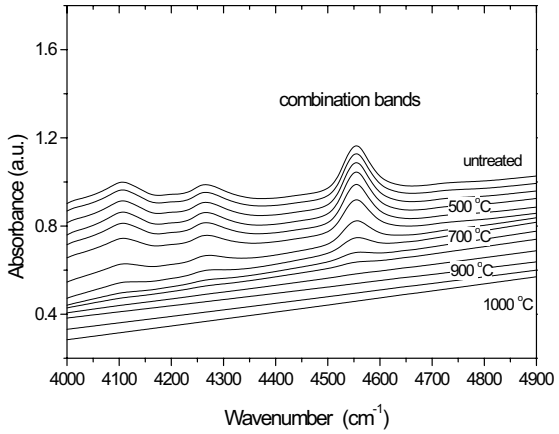

FIGURE 4. Temperature evolution of spectra (4000–4900 cm^{-1}) of combination bands of OH^- species and vibrational phonons (data from thin sections).

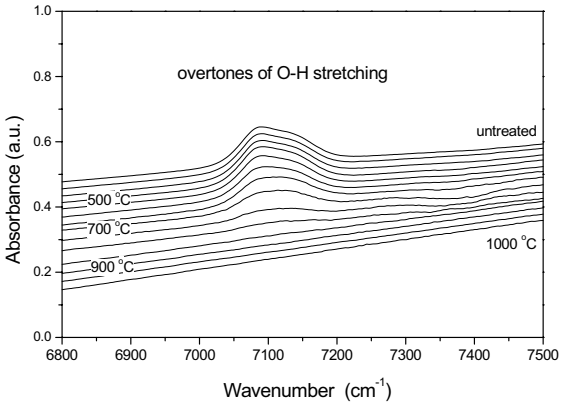

FIGURE 5. Temperature evolution of IR spectra (6800–7500 cm^{-1}) of the first overtones of the O-H stretching bands (data from thin sections).

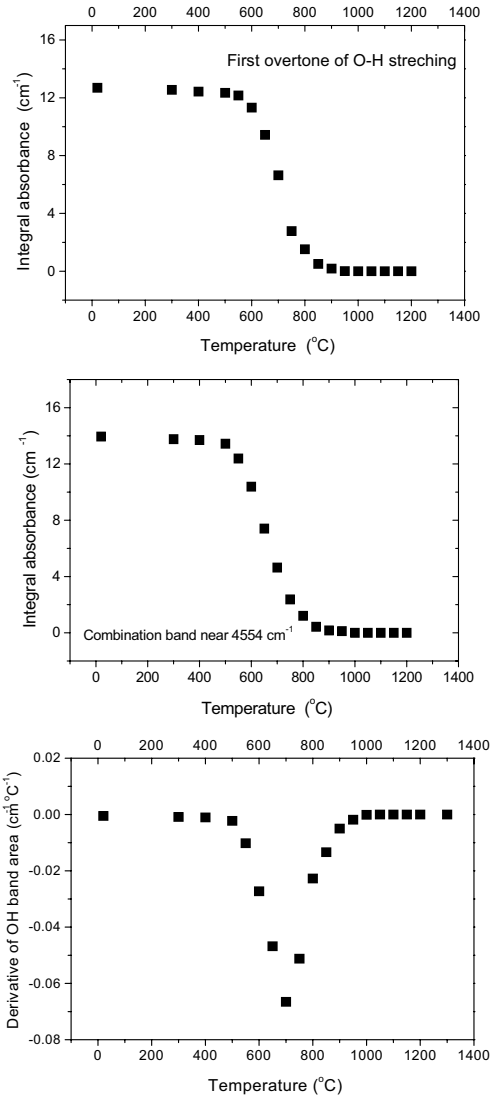

FIGURE 6. (**a**) Temperature dependence of integral absorbance of first overtone bands of OH^- species, (**b**) temperature dependence of integral absorbance of the combination bands of OH^- species, and (**c**) change (derivative) of integrated absorbance of the overtone bands as a function of temperature. The errors are smaller than the symbol sizes.

with the original layered framework is preserved in the sericite dehydroxylate. Most phonon bands of sericite show a general decrease in frequency upon dehydroxylation. The peak positions of the observed IR bands (obtained using the second derivative method) between 20 and 1200 cm^{-1} are plotted as a function of annealing temperature (Fig. 7). The value of the relative changes in frequency varies with different types of vibrational bands. The Si-O stretching bands between 900 and 1200 cm^{-1} show a complex band-splitting-like behavior with dehydroxylation (Figs. 1b and 7). For example, the band near 1065 cm^{-1} apparently becomes two well-separated bands peaking at 1046 and 1071 cm^{-1}. This change indicates a complex local modification related to the SiO_4 ions and could also suggest a change of site symmetries and further lifting of the triply degenerate stretching vibrations of the SiO_4 ions, or distorted structural ions. Our observations are consistent with those of Udagawa et al. (1974) and Guggenheim et al. (1987), who showed that although the averaged Si-O bond distances in muscovite and its dehydroxylate are similar, some of Si-O bonds become longer whereas others become shorter or are almost unchanged. The spectral changes seen in the present study reflect the complex structural variations. During dehydroxylation, an oxygen atom adjacent to the octahedral aluminum site is lost, which leads to a change from six-coordinated aluminum to a fivefold coordination environment (Mackenzie et al. 1987) and a change in the bond valence to the five O atoms of the oxygen-aluminum polyhedron. Consequently, readjustment of the bond distances between T and the non-bridging or bridging oxygen atom occurs to preserve the charge on the tetrahedrally coordinated cation, and as a result a lower local symmetry and band splitting may occur. Our data show that the bending bands associated with the SiO_4 and original AlO_6 polyhedra between 300 and 550 cm^{-1} exhibit weak frequency changes. In contrast, the IR bands associated with K-O vibrations showed the largest relative change. The dehydroxylation led to a systematic decrease in intensity for K-O vibrations at 141, 168, and 191 cm^{-1}. In fact, the 168 and 191 cm^{-1} bands became weak local maxima in the sericite dehydroxylate. The K-O vibrational bands near 141, 168, and 191 cm^{-1} in sericite shifted to 136, 159, and 186 cm^{-1} (with relative changes of ~4, ~5, and ~3%, respectively) in the sericite dehydroxylate. In comparison with the change of ~4% in the out-of-plane K-O vibration near 141 cm^{-1}, the in-plane K-O vibration, which peaked at 111 cm^{-1} with the lowest phonon frequency, showed a much larger change in frequency (~8%). It shifted or "softened" to 102 cm^{-1} in the sample treated at 1100 °C and became a broad feature that appears to consist of more than one band. This implies that in sericite dehydroxylate the cation has a more distorted local environment. The systematic decrease in these phonon frequencies indicates a weakening of the bond strengths that are directly related to bond distances and valence states of the atoms involved. Our data agree with the results of the X-ray diffraction study of Udagawa et al. (1974). These authors showed that the average of the two types of K-O distances increased from 2.87 and 3.35 Å in muscovite to 2.96 and 3.38 Å in muscovite dehydroxylate, respectively. The general decrease of phonon frequencies of sericite indicates a weakening or a "softening" of structural bonding, responsible for the reported dehydroxylation-induced increase in the cell volume (from 935.8 to 971.2 $Å^3$, ~4% expansion) (Udagawa et al. 1974; Guggenheim et al. 1987).

The incorporation of CO_2 into the heat-treated sericite is evidenced by the weak IR signal that gradually develops near 2345 cm^{-1} (Figs. 2 and 8), which is attributed to the anti-symmetric stretching (ν_3) of molecular CO_2 (Fine and Stolper 1985; Mysen 1976). This characteristic band was absent in the starting material, and it became detectable around 400 °C. Its frequency showed an increase (from 2345 cm^{-1} at 500 °C to 2349 cm^{-1} at 800 °C) upon heating. One of the important questions related to the structurally incorporated CO_2 is the origin of these carbon atoms. The possibilities are that they originate from the high-temperature decomposition of internal carbon substances pre-existing in the starting material, or diffusion of carbon species produced in firing, or a combination of both. For the former case, the decomposition or dissociation of CO_3^{2-} ions could be a potential mechanism. The dissociation of CO_3^{2-} ions and occurrence of incorporated CO_2 during heating have been well documented (e.g., in apatite, Dowker and Elliottt 1983). CO_3^{2-} ions generally show strong C-

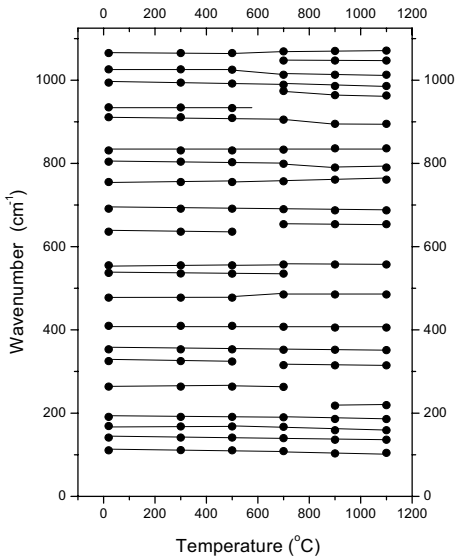

FIGURE 7. Phonon peak positions as a function of temperature. The errors are smaller than the symbol sizes.

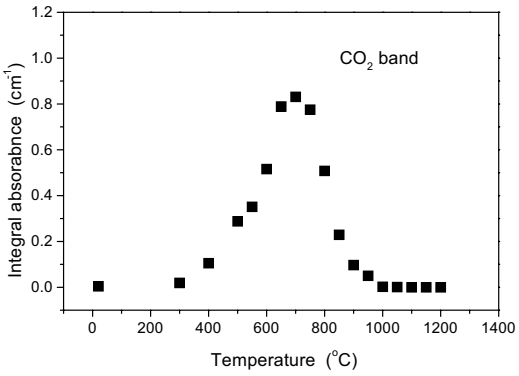

FIGURE 8. Temperature dependence of integral absorbance of the CO_2 signal near 2345 cm^{-1}.

O stretching bands near 1450 cm^{-1} (ν_3 vibrations) in IR spectra (White 1974; Nakamoto 1978). Our data do not support the idea that CO_2 originated from dissociation of CO_3^{2-} ions that existed in the starting material, because of the absence of the characteristic bands of CO_3^{2-} (Fig. 1c), although the species could be present as trace substances in minerals. We were also surprised to find that weak bands near 1462 and 1473 cm^{-1} indicating CO_3^{2-} ions were clearly detected in the powdered sample annealed at 500 and 700 °C (we did not attempt to measure CO_3^{2-} absorption in the fired thin sections, because the samples showed complex multi-phonon absorption in the wavenumber region), where CO_2 also appeared. On further heating, the CO_3^{2-} feature disappeared above 900 °C, where CO_2 also became almost undetectable. This shows that the formation of CO_2 is not at the cost of CO_3^{2-} and this also supports our conclusion that the incorporated CO_2 does not originate from dissociation of CO_3^{2-}. Comparing the data on carbon-related species obtained from annealed sericite with those from heat-treated pyrophyllite (Wang et al. 2003), we noted two differences: (1) CO_3^{2-} was not detected in the heated pyrophyllite, but CO was detected (at a higher temperature, 850 °C) and (2) under the same experimental conditions (e.g., thin sections, annealing time of 15 min), the temperature at which the concentration of CO_2 in sericite reaches a maximum is relatively low (~700 °C), in contrast to ~800 °C for pyrophyllite. The appearance of these CO_2, CO_3^{2-}, and some OH^- bands at temperatures as low as 400–500 °C leads us to speculate that low concentrations of other C-H species (e.g., CHn) could be present in the untreated sample. These species could be associated with the weak band near 3444 cm^{-1} (Figs. 3a and 3b). They might break down at relatively low temperatures and partially or fully contribute to the observed spectral anomalies (i.e., the extra CO_2, CO_3^{2-}, and OH^-) near 500 °C. The potential occurrence of macro-fractures or cracks during heating may play a role (e.g., speeding up the diffusion process of CO_2 or CO) in CO_2 incorporation during high-temperature experiments. However, this is unlikely the dominant factor; CO_2 in cracks is not expected to give the systematic change of intensity observed in this study. Furthermore, CO_2 trapped in cracks is expected to appear as free gaseous molecules and should show a peak with a constant wavenumber, as well as changes in the spectra associated with out-gassing in the vacuum chamber.

To determine whether the carbonization process in sericite is related to the dehydroxylation process and to explore their possible relationship in a quantitative way, the integral absorbance (i.e., IR band area) and the derivative of the integral of the OH^- species were plotted against the IR band area of CO_2 (Figs. 9a and 9b). The data in Figure 9a form a curve, which implies that the two processes are not completely independent, otherwise one would expect randomly scattered data points. The results shown in Figure 9b further confirm that the CO_2 incorporation process is associated with the change or the loss rate of the OH concentration (Fig. 9b), a direct result of the thermally induced structural change. During the experiments, we noted that there was a systematic change of sample color with varying temperature. The samples first became light grey near 500 °C, then grey and white on further heating. The change of color might be associated with carbon species and also the thermally induced oxidation of some cations.

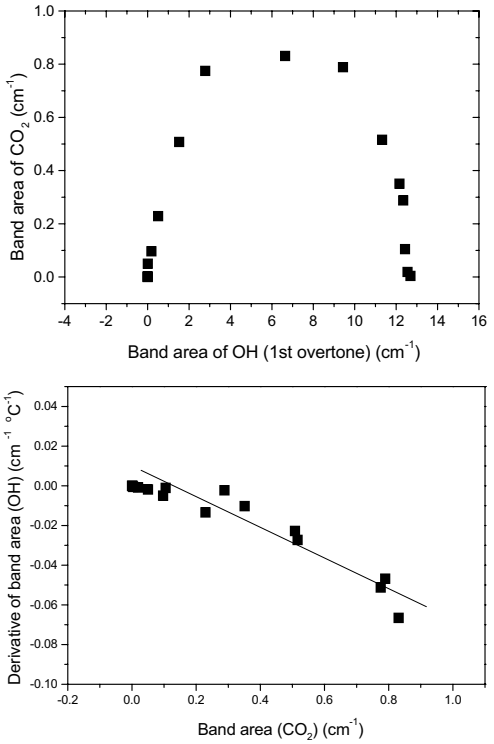

FIGURE 9. (**a**) Plot of integral intensity (band area) of CO_2 as a function of integral intensity (band area) of OH^- species (first overtones), and (**b**) comparison of the change (derivative) of the OH band area and the band area of CO_2. The line is a visual guide.

DISCUSSION

It is instructive to compare our IR data with existing thermogravimetric (TG) measurements to gain a better understanding of what happens at the atomic level during dehydroxylation. As described earlier, our IR analysis shows that the dehydroxylation process is characterized by a dramatic decrease in the intensity of the O-H stretching bands between 3630 and 3660 cm^{-1} (Fig. 1b). The derivative of the integral absorbance of these bands exhibits a minimum near 700 °C (Fig. 6c) indicating a maximum loss rate. In comparison, investigations based on weight loss measurements showed the greatest loss between 600 and 850 °C (e.g., Hanykýř et al. 1985; Kristóf et al. 1985; Guggenheim et al. 1987; Wang 1999), although slightly different dehydroxylation temperature(s) were reported in different studies. The sericite sample used in the present study appears similar, in terms of chemical composition, to the muscovite sample investigated by Guggenheim et al. (1987) and the sericite sample (from Guangnin, Guangdong, China) studied by Wang (1999). Wang (1999) reported a chemical composition for the Guangnin sericite (in wt%) of 46.68 SiO_2, 0.20 TiO_2, 36.69 Al_2O_3, 0.22 Fe_2O_3, 0.10 FeO, 0.64 MgO, 0.20 CaO, 0.35 Na_2O, 10.24 K_2O, 4.12 H_2O, and negligible amounts of other elements such as Mn and P. The TG and DTA data of Wang (1999) showed water loss of 2.2% peaking at 707 °C and 1.4 % at 903 °C, suggesting a two-stage dehydroxylation process. In comparison with our IR results, the water loss near 700 °C is mainly associated with OH^- species near 3630, 3645, and 3660 cm^{-1} (Fig. 1b), which are present in the untreated material. These

species exhibited a decrease in intensity on heating above 550 °C and a maximum loss near 700 °C. On further heating these OH^- species became undetectable at 900 °C (Figs. 3–6). During dehydroxylation, the O-H bonds associated with the species are broken, and H_2O molecules form and are driven out the sample. It is worth noting that the 2.2% weight loss recorded near 700 °C by TG and DTG (e.g., Wang 1999) may not fully reflect the thermal behavior of these bands, as OH^- bands near 3480 and 3570 cm^{-1} developed during heating. Some type of proton migration or possible partial dehydroxylation-induced formation of the new OH^- sites must be involved. The other issue that could complicate interpretation of the 2.2% loss is the incorporation of CO_2 and CO_3^{2-} into the heated sample. Both the OH^- and CO_2 species showed maximum intensities near 700 °C. Their occurrence and variations with temperature would undoubtedly influence the outcome of the weight loss analysis. In this respect, we believe the weight loss data reflect the average change that is affected by the thermal behaviors of all these different types of species. We shall further discuss the possible causes for the weight loss near 900 °C reported in the Guangnin sericite. As our IR data showed that the characteristic hydroxyl bands (i.e., those bands near 3630, 3645, and 3660 cm^{-1}) of sericite disappeared below 900 °C, they should make no significant contributions to the 1.4% weight loss seen near 900 °C in the TG and DTA measurements of Wang (1999). Clearly, the species which are responsible for the loss must persist between 700 and 900 °C and eventually vanish on further heating. Based on our IR data, there at least three types of absorption bands which meet the criteria: the thermally developed hydroxyl bands (near 3480 and 3570 cm^{-1}), the CO_2 band near 2345 cm^{-1}, and the CO_3^{2-} bands near 1462 and 1473 cm^{-1}. We did not attempt to determine the concentrations of these additional species because of the lack of calibrations for these thermally generated new components (especially for CO_2) and the lack of understanding on how the CO_2 was incorporated into the heated sample. Using a calibration based on sodium aluminosilicate glasses (Fine and Stolper 1985), Wang et al. (2003) estimated the CO_2 concentration (~0.01 wt% CO_2) for a pyrophyllite sample heated at 750 °C for 1 h. In the heat-treated sericite sample the CO^2 concentration could be of a similar order of magnitude as the CO_2 absorption showed similar intensity. The relatively weak signals from these carbon species in heated sericite make us question whether these signals are partially or fully responsible for the ~1.4 % weight loss near 900 °C and whether other (undetected) species are also involved. Our IR data are more consistent with the TGA and DTG data for muscovite reported by Guggenheim et al. (1987), who showed a single and relatively broad peak near ~700 °C. The relatively broad feature can be associated with the complex combination of the dehydroxylation of the original OH^- species, the formation of thermally induced or developed OH^- and CO_2 species, and the disappearance of these components.

Our observation of carbonization in the heated sample has some interesting implications. Firstly, the occurrence of thermally induced CO_2 and CO_3^{2-}, the development of OH^- species, and their disappearance at high temperatures indicates that the partial sericite dehydroxylate has a local configuration, strictly speaking, different from that of sericite and the dehydroxylate, and it can accommodate the new species. The appearance of these species is the result of proton migration and carbon diffusion, and it can be affected by different processes. Because of the relatively low intensities associated with these additional species, we consider that they generate local defects and distortions, but they might not significantly affect the whole layer structure of the sericite dehydroxylate. Secondly, one interesting question raised by our observation is whether the extra CO_2 and the developed OH^- species are structurally linked, or whether they are both required in the partial dehydroxylation state. Our data appear to suggest otherwise, because the hydroxyl band near 3480 cm^{-1} remained clearly visible at 1100 °C, whereas the CO_2 absorption near 2345 cm^{-1} became almost undetectable beyond 900 °C. This means that the OH^- and CO_2 species are not directly structurally linked or stabilized by each other. In terms of a possible application of our observation, we wonder whether the presence of these new species could be used as an indication for samples that might have undergone natural high-temperature events.

ACKNOWLEDGMENTS

The manuscript benefited from reviews by J.-L. Robert and M. Nowak, and comments from Associate Editor, S. Kohn.

REFERENCES CITED

Aines, R.D. and Rossman, G.R. (1985) The high temperature behaviour of trace hydrous components in silicate minerals. American Mineralogist, 70, 1169–1179.

Béarat, H., McKelvy, M.J., Chizmeshya, A.V.G., Sharma, R., and Carpenter, R.W. (2002) Magnesium hydroxide dehydroxylation/carbonation reaction processes: implications for carbon dioxide mineral sequestration. Journal of the American Ceramic Society, 85, 742–748.

Beran, A. (2002) Infrared spectroscopy of micas. In A. Mottana, F.P. Sassi, J.B. Thompson, Jr., and S. Guggenheim, Eds., Micas: Crystal Chemistry and Metamorphic Petrology, 46, 351–369. Reviews in Mineralogy and Geochemistry, Mineralogical Society of America, Washington, D.C.

Brooker, R.A., Kohn, S.C., Holloway, J.R., McMillian, P.F., and Carroll, M.R. (1999) Solubility, speciation and dissolution mechanisms for CO_2 in melts on SiO_2-$NaAlO_2$ join. Geochimica et Cosmochimica Acta, 63, 3549–3565.

Brooker, R.A., Kohn, S.C., Holloway, J.R., and McMillian, P.F. (2001) Structural controls on the solubility of CO_2 in silicate melts Part II: IR characteristics of carbonate groups in silicate glasses. Chemical Geology, 174, 241–254.

Copeland, P. and Harrison, T.M (1990) Episodic rapid uplift in the Himalaya revealed by $^{40}Ar/^{39}Ar$ analysis of detrital K-feldspar and muscovite, Bengal fan. Geology, 18, 354–357.

Deer, W.A., Howie, R.A., and Zussman, J. (1992) An introduction to the rock-forming minerals, 2nd ed., 696 pp. Longman Scientific & Technical.

Diaz, M., Farmer, V.C., and Prost, R. (2000) Characterization and assignment of far infrared absorption bands of K^+ in muscovite. Clays and Clay Minerals, 48, 433–438.

Diaz, M., Laperche, V., Harsh, J., and Prost, R. (2002) Far infrared spectra of K^+ in dioctahedral and trioctahedral mixed-layer minerals. American Mineralogist, 87, 1207–1214.

Dowker, S.E.P. and Elliottt, J.C. (1983) Infrared study of trapped carbon-dioxide in thermally treated apatites. Journal of Solid State Chemistry, 47, 164–173.

Drits, V.A., Besson, G., and Muller, F. (1995) An improved model for structural transformations of heat-treated aluminous dioctahedral 2:1 layer silicates. Clays and Clay Minerals, 43, 718–731.

Farmer, V.C. (1974) The layer silicates. In V.C. Farmer, Ed., The infrared spectra of minerals, 539 pp. Mineralogical Society, London.

Farmer, V.C. and Russell, J.D. (1964) The infra-red spectra of layer silicates. Spectrochimica Acta, 20, 1149–1179.

Fine, G. and Stolper, E. (1985) The speciation of carbon dioxide in sodium aluminosilicate glasses. Contributions to Mineralogy and Petrology, 91, 105–121.

Fitzgerald, J.J., Hamza, A.I., Dec, S.F., and Bronnimann, C.E. (1996) Solid-state ^{27}Al and ^{29}Si NMR and ^{1}H CRAMPS studies of the 2:1 phyllosilicate pyrophyllite. Journal of Physical Chemistry, 100, 17351–17360.

Gaines, G.L. Jr. and Vedder, W. (1964) Dehydroxylation of muscovite. Nature, 201, 495.

Glasmacher, U.A., Langb, M., Klemmec, S., Moined, B., Barberoe, L., Neumannb, R., and Wagner, G.A. (2003) Alpha-recoil tracks in natural dark mica: Dating geological samples by optical and scanning force microscopy. Nuclear Instruments and Methods in Physics Research Section B: Beam Interactions with Materials and Atoms, 209, 351–356.

Guggenheim, S., Chang, Yu-Hwa, and Koster van Groos, A.F. (1987) Muscovite dehydroxylation: High-temperature studies. American Mineralogist, 72, 537–550.

Hanykýř. V., Ederová, J., Trávníček, Z., and Šrank, J. (1985) Isothermal dehydroxylation of muscovite mica. Thermochimica Acta, 93, 517–520.

Hashemi-Nezhad, S.R. and Durrani, S.A. (1981) Registration of alpha-recoil tracks in mica: The prospects for alpha-recoil dating method. Nuclear Track Detection, 5, 189–205.

Ishii, M., Shimanouchi, T., and Nakahirea, M. (1967) Far infrared absorption spectra of layer silicates. Inorganica Chimica Acta, 1, 387–392.

Kapoor, B.S., Singh, H.B., Goswami, S.C., Abrol, I.P., Bhargava, G.P., and Pal, D.K. (1981) Weathering of micaceous minerals in some salt-affected soils. Journal of the Indian Society of Soil Science, 29, 486–492.

Kristóf, J., Vassányi, I., Nemecz, E., and Inczédy, J. (1985) Study of the dehydroxylation of clay minerals using continuous selective water detector. Thermochimica Acta, 93, 625–628.

Langer, K., Chatterjee, N.D., and Abraham, K (1981) Infrared studies of some synthetic and $2M_1$ dioctahedral micas. Neues Jahrbuch fur Mineralogie, Abhandlungen, 142, 91–110.

Laperche, V. and Prost, R. (1991) Assignment of the far-infrared absorption-bands of K in micas. Clays and Clay Minerals, 39, 281–289.

MacKenzie, K.J.D., Brown, I.W.M., Meinhold, R.H., and Bowden, M.E.J. (1985) Thermal reactions of pyrophyllite studied by high-resolution solid-state ^{27}Al and ^{29}Si nuclear magnetic resonance spectroscopy. Journal of the American Ceramic Society, 68, 266–272.

MacKenzie, K.J.D., Brown, I.W.M., Cardile, C.M., and Meinhold, R.H. (1987) The thermal reactions of muscovite studied by high-resolution solid-state ^{29}Si and ^{27}Al NMR. Journal of Materials Science, 22, 2645–2654.

Mckeown, D.A., Bell, M.L., and Etz, E. (1999) Raman spectra and vibrational analysis of the trioctahedral mica phlogopite. American Mineralogist, 84, 970–976.

Morizet, Y., Brooker, R.A., and Kohn, S.C. (2002) CO_2 in halpo-phonolitic melt: solubility, speciation and carbonate complexation. Geochimica et Cosmochimica Acta, 66, 1809–1820.

Muller, F., Drits, V., Plançon, A., and Robert, J-L. (2000) Structural Transformation of 2:1 dioctahedral layer silicates during dehydroxylation-rehydroxylation reactions. Clays and Clay Minerals, 48, 572–585.

Mysen, B.O. (1976) The role of volatiles in silicate melts: Solubility of carbon dioxide and water in feldspar, pyroxene and feldspathoid melts to 30 Kb and 1625 °C. American Journal of Science, 276, 969–996.

Nakamoto, K. (1978) Infrared and Raman spectra of inorganic and coordination compounds, 448 pp. Wiley, New York.

Pei, F.M. and Shi, Y. (1996) Geological characteristics of the sericite deposits in Xiling, Song County and preliminary analysis of its genesis. Henan Geology, 14, 160–167.

Plank, H., Resel, R., Sitterb, H., Andreevb, A., Sariciftcic, N. S., Hlawacekd, G., Teichertd, C., Thierrye, A., and Lotz, B. (2003) Molecular alignments in sexiphenyl thin films epitaxially grown on muscovite. Thin Solid Films, 443, 108–114.

Ray, S.S. and Okamoto, M. (2003) Polymer/layered silicate nanocomposite: a review from preparation to processing. Progress in Polymer Sciences, 28, 1539–1641.

Robert, J.-L., Beny, J.M., Dellaventura, G., and Hardy, M. (1993) Fluorine in micas – crystal-chemical control of the OH-F distribution between trioctahedral and dioctahedral sites. European Journal of Mineralogy, 5, 7–18.

Taylor, W.R. (1990) The dissolved $(CO_3)^{2-}$ in alumino-silicate melts—Infrared spectroscopic constraints on the cationic environment of dissolved $(CO_3)^{2-}$. European Journal of Mineralogy, 2, 547–563.

Taylor, A.S., Blumb, J.D., Lasaga, A.C., and MacInnis, I.N. (2000) Kinetics of dissolution and Sr release during biotite and phlogopite weathering. Geochimica et Cosmochimica Acta, 64, 1191–1208.

Udagawa, S., Urabe, K., and Hasu, H. (1974) The crystal structure of muscovite dehydroxylate. Japanese Association of Mineralogists, Petrologists, and Economic Geologists, 69, 381–389.

Wang, D.Q. (1999) Study on mineralogical properties of mica minerals and the effect of K release. Ph.D. thesis, Institute of Geology, Chinese Academy of Sciences, Beijing.

Wang, L., Zhang, M., Redfern, S.A.T., and Zhang, Z.Y. (2002) Dehydroxylation and transformations of the 2:1 phyllosilicate pyrophyllite at elevated temperatures: An infrared spectroscopic study. Clays and Clay Minerals, 50, 272–283.

Wang, L., Zhang, M., and Redfern, S.A.T. (2003) Infrared study of CO_2 incorporation into pyrophyllite $[Al_2Si_4O_{10}(OH)_2]$ during dehydroxylation. Clays and Clay Minerals, 51, 439–444.

White, B.W. (1974) The carbonate minerals. In W.C. Farmer, Ed., The Infrared Spectra of Minerals, p. 227–284. Mineralogical Society of London.

Zhang, M., Wruck, B., Graeme-Barber, A., Salje, E.K.H., and Carpenter, M.A. (1996) Phonon spectra of alkali-feldspars: phase transitions and solid solutions. American Mineralogist, 81, 92–104.

MANUSCRIPT RECEIVED JANUARY 30, 2004
MANUSCRIPT ACCEPTED MAY 27, 2004
MANUSCRIPT HANDLED BY SIMON KOHN